Journal of Surgery
De Masi M, et al. J Surg 8: 1840
www.doi.org/10.29011/2575-9760.001840
www.gavinpublishers.com
Research Article

# Thoracic Aorta Remodeling after TEVAR: Monitoring Morphological Parameters to Predict Unfavorable Evolution

**Mariangela De Masi[1,2*], Carine Guivier-Curien[2], Mohamed Boucekine[3], Pierre Antoine Barral[4], Laurence Bal[1], Virgile Omnes[1], Marine Gaudry[1], Alexis Jacquier[4], Philippe Piquet[1] and Valérie Deplano[2]**

[1]Department of Vascular Surgery, Timone Aortic Center, APHM, Timone Hospital, 13005 Marseille, France

[2]CNRS, Centrale Marseille, IRPHE, Aix Marseille University, 13013 Marseille, France

[3]Aix Marseille Univ, CEReSS EA3279, 13005 Marseille, France

[4]Department of Radiology, APHM, Timone Hospital, 13005 Marseille, France

[*]**Corresponding author:** Mariangela De Masi, Department of Vascular Surgery, Timone Aortic Center, APHM- Timone Hospital, 13005 Marseille, France

**Citation:** De Masi M, Guivier-Curien C, Boucekine M, Barral PA, et al. (2023) Thoracic Aorta Remodeling after TEVAR: Monitoring Morphological Parameters to Predict Unfavorable Evolution. J Surg 8: 1840 DOI: 10.29011/2575-9760.001840

**Received Date:** 29 June, 2023; **Accepted Date:** 04 July, 2023; **Published Date:** 07 July, 2023

## Abstract

**Background**: The aim of this study was to assess geometrical modifications of the aneurysmal Thoracic Aorta (TA) after Thoracic Endovascular Repair (TEVAR) over 3 years of follow-up, to identify features predicting unfavorable evolution.

**Methods:** Twenty-five patients treated by TEVAR for an atheromatous thoracic aortic aneurysm were retrospectively included in a single center study. All patients had clinical and radiological follow up for 3 years post TEVAR allowing defining patient with a Favorable Aortic Evolution (FAG) or an Unfavorable (UBG) evolution. Four Computed Tomography Angiographies (CTA) were analyzed: preoperative CTA (T0) and 3 postoperative: 6-12 months (T6), 24 months (T24) and 36 months (T36), allowing extraction of lengths, angles, tortuosity indexes, and diameters for each segment of the thoracic aorta. Descriptive and bayesian statistical methods were used to express results and assess the link between geometrical parameters and the risk of poor outcome at each post-operative follow-up time.

**Results:** At T0, none of these geometrical parameters is associated with a risk of unfavourable evolution. On the other hand, TA length, angle, and tortuosity index between T0 and T6 showed a significant increase in UBG (respectively 22.3±5.1 mm, 23.8±7.2° and 0.1±0.01 compared to a stability in FAG 0.01±0.05mm, -1±0.9°, 0.01±0.02 respectively; $p<0.05$). Similar results are found for later time point.

**Conclusions:** Quantifying the post-TEVAR temporal evolution of TA geometrical parameters as early as 6 months discriminates favourable from unfavourable aortic evolution.

**Keywords:** Aneurysm; Bayesian approaches; Follow-up period; Morphological parameters; Thoracic aorta remodeling

**Abbreviations:** BCT: Brachiocephalic Trunck; BSA: Body Surface Area; CAOD: Coronary Artery Occlusive Disease; CL: Centerline; COPD: Chronic Occlusive Pulmonary Disease; CTA: Computed Tomography Angiography; EP: Endoprosthesis; FAG: Favourable A Group; LCCA: Left Common Carotid Artery; LSCA: Left Subclavian Artery; MCMs: Multidisciplinary Consultation Meetings; T0: Preoperative Time; T6: Post-Operatives Scanner at 6 or 12 Months; T24: Post-Operatives Scanner at 24 Months; T36: Post-Operatives Scanner at 36 Months; TA: Thoracic Aorta; TAA: Thoracic Aortic Aneurysm; TEVAR: Thoracic Endovasclar Aortic Repair; UBG: Unfavorable B Group

## Introduction

Thoracic Endovascular Aortic Repair (TEVAR) has been shown to be a safe and effective treatment for different aortic pathologies, outstripping open surgery as the primary approach [1]. The post TEVAR aortic remodeling is due to the natural aging process, disease progression, and endoprosthesis radial forces and it has been confirmed as critical in determining treatment durability [2]. Other investigators have extensively described the importance of the aortic anatomy (angulation, diameter, tortuosity) and their relationship with endoleaks in different aortic pathologies, but these studies mainly considered a short follow-up period [3-5]. Several reports describing heterogeneous pathologic processes indicate that endoleaks are associated with anatomic factors, such as the diameter of the residual aneurysm, the radius of the aortic curve, and the tortuosity of the aorta [2,6,7]. But maximal diameter, maximal diameter evolutions over time as well as endoleak apparition remain the main parameters to unfavorable aortic remodeling after TEVAR. The insertion of the endoprosthesis in an aneurysm sac may promote adverse aortic remodeling because the stent graft is less compliant than the normal aortic tissue [8,9]. Not all patients will experience the same evolution of thoracic aorta remodeling and risk of endoprosthesis failure after TEVAR. Assessing remodeling progression should enable clinicians to better predict which patients are at higher risk of aortic complications, allowing them to provide a better and earlier patient-specific treatment [10].

The aim of this study was, 1) to describe a framework of medical image analysis to quantify geometrical thoracic aorta changes during the first three years after TEVAR 2) To assess the value of several geometrical parameters to predict unfavorable aortic remodeling earlier than reference parameters (i.e., diameter and diameter progression).

## Materials and Methods

The study was conducted in accordance with the Declaration of Helsinki and RGPD Law. This restrospective study follows the MR004 rules and local agreement was obtained # PADS23-17 on 6 October 2021.

### Study Design and Patients Sample

A retrospective analysis was conducted of twenty-five patients who were treated with thoracic stent-graft at a single center for thoracic aortic aneurysm, with the following inclusion criterions: availability of a preoperative computed tomography angiography (CTA) (T0) and 3 postoperative CTA performed 6 to 12 months (T6), 24 months (T24) and 36 months (T36) after surgery and availability of all clinical information for a follow up covering at least 36 months after surgery. Only patient with atherosclerotic aneurysm were included. Patients with a missing CTA (T0, T6, T24 or T36) or lost of view for medical follow-up or aneurysm of a non-atherosclerotic origin were excluded. Favorable A group (FAG) was define by the association of 2 parameters: patient without significant aortic diameter increase (maximal aortic diameter increase <10mm / 3 years) and patients who did not require an aortic reintervention during follow-up. On the other hand, patient who required aortic reinterventions as additional treatment related to the thoracic aorta or any direct complication of the initial TEVAR procedure were included in an unfavorable B group (UBG). All the TEVAR procedures were performed using the following stents-graft: GORE Conformable TAG (W. L. Gore & Associates, Flagstaff, Arizona), Cook (Cook Medical, Bloomington, IN, USA) and Medtronic (ValiantTM or the Valiant CAPTIVIA generation). The diameter of stent-graft was oversized by 15% to 20% according to pre intervention CTA measurements. The mean of the three diameter measurements for each proximal and distal landing zone was subtracted from the nominal device diameter and then divided by the mean diameter of the landing zone to calculate the endoprosthesis oversizing. The proximal and distal anchoring zone was recorded according to Ishimaru's classification modified by Criado [6,7]. Proximal and distal sealing zones of at least 20 mm along the aortic centre line was selected in normal thoracic aorta, defined by an aortic wall with no evidence of thrombus, calcification or excessive angulation with a diameter lower than 40mm. The overlap between 2 stent graft was ≥ 3 cm if second device was one or two sizes larger than the first device. The overlap was ≥ 5 cm if second device was the same

size. Prophylactic lumbar drainage and revascularization of the supraaortic trunk vessels was discussed during Multidisciplinary Consultation Meetings (MCMs) before surgery and according to international guidelines and multidisciplinary expertise.

### Image Acquisition and 3D Geometric Analysis

CTA (see Supplemental Appendix 1 for details) was performed on a multi-detector 64-row scanner (REVO EVO, General Electric Healthcare, Buc, France) after contrast media injection with standard parameters. All CTAs (T0, T6, T24, T36) were transferred on a workstation equiped with a vascular imaging software (Endosize; Therenva, Rennes, France). The first step of image analysis was the manual extraction of a three dimensional (3D) arterial Lumen Centerline (CL) starting by a manual designation of the proximal and distal ends of the thoracic aorta from sinotubular junction to celiac trunk allowing the automatic creation of a 3D aortic CL (Figure 1A). Spatial coordinates (x,y,z) of CL points were exported every mm. The aorta was divided into five anatomic zones, from zone 0 to zone 4 according to Ishimaru's classification modified by Criado [6,7,11]. Points of the CL that crosses limits between two successive zones were defined as follows: P0 for the first point at the sinotubular junction, P1 between Z0 and Z1, P2 between Z1 and Z2, P3 between Z2 and Z3, P4 between Z3 and Z4, and P5 at the end of Z4 (Figure 1B).

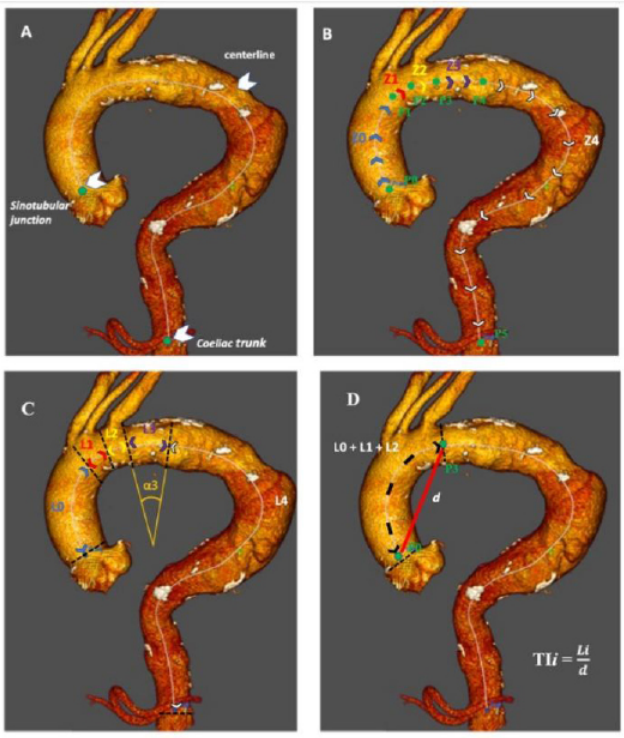


**Figure 1.** Image A illustrates the centerline created from the sinotubular junction to the coeliac trunk. Image B shows the points (P0 to P5) used to define the cross-sections of the aortic lumen and length of the successive zones (Z0 to Z4). Image C shows an example of measurements of angles (α*3*). Image D shows an example of tortuosity measurement (TI) from Z0 to Z2.

### Definition of the Geometrical Parameters

Centerline was used to define aortic length, angle, and tortuosity in the 5 predefined zones (Figure 1B).

**Lengths:** L0, L1, L2, L3 and L4 were defined respectively as the length of Z0, Z1, Z2, Z3, and Z4 along the CL. The length Li_j corresponded to the length from the beginning of zone Zi to the end of zone Zj. The sum of all lengths (L0+L1+L2+L3+L4) defined the length of the thoracic aorta (L_ATot). The lengths of proximal and distal neck (Lpn and Ldn respectively), as well as the length of the entire endoprothesis (L_EP), were measured (Figure 1C).

**Aortic Angulation:** α0, α1, α2, α3, and α4 were the angles between planes perpendicular to the CL at the points marking the start (Pi) and end (Pi+1) of each zone. The angle αi_j corresponded to the angle from the beginning of zone Zi to the end of zone Zj. Angles between start and end of the proximal and distal neck of the aneurysm (αpn, and αdn respectively), the angulation of the entire endoprothesis (α_EP), and overall aortic angulation of the whole thoracic aorta (α_ATot) were also assessed. (Figure 1C)

**Tortuosity Index:** TIi $= \frac{L_i}{d_i}$ reflected the tortuosity of a Zi zone, defined by dividing the length of the zone Li by the spatial straight distance di ( $d_i = \overline{[Pi;\ Pi+1]}$) between the start point (Pi) and the end point (Pi+1) of Zi. The overall tortuosity of the aortic arch (TI0_2) (Figure 1D) and of the descending aorta (TI3_4) were considered for statistical analysis. The tortuosity index of the entire endoprosthesis (TI_EP) was also assessed. Finally, overall tortuosity of the aorta (TI_ATot) was evaluated by dividing L_ATot by spatial straight distance between proximal and distal ends of the whole CL ($\overline{[P0;P5]}$).

**Diameters:** Maximal aortic diameter was assessed perpendicular to the CL and including aortic thrombus and aortic wall. There were automatically computed by the post-processing tool and corrected, if necessary, by the reader. D0, D1, D2, D3 and D4, were the maximal aortic diameters at P0, P1, P2, P3, P4, respectively. Diameters of proximal and distal necks of the aneurysm (Dpn and Dpn respectively), and maximal aneurysm diameter, Daneurysm, were also measured.

### Statistical Analysis

Values are expressed in mean and range. Bayesian Gaussian logistic regression and linear parametric approaches were therefore

chosen for their ability to treat small populations (see Supplemental Appendix 2 for implementation details and references). The first model (Bayesian logistic regression) is performed to evaluate the associations between unfavorable outcomes and geometrical explanatory variables at preoperative (T0) and postoperative stages (T6, T24, and T36). When an odd ratio (OR) is higher than 1, the risk of poor outcome increases whereas an OR < 1 is predictive of good outcome. The results are significative if the 95% confidence interval ($CI_{95\%}$) does not include 1 value.

The second model (Bayesian linear) is performed to compare the evolution of each morphological and geometrical parameter between pre and each postoperative time in FAG and UBG. Mean temporal evolution for each group is estimated and the difference between UBG mean temporal evolution value and FAG mean temporal evolution value is reported ($\beta_1$ values). The 95% confidence interval ($CI_{95\%}$) is calculated for the $\beta_1$ value of group variable. If the confidence interval does not include the null value, we conclude that there is a statistically significant difference in the temporal evolution between the groups.

To compare the means between group and temporal evolution of the means between UBG and FAG groups, a two-way analysis of variance (ANOVA) was used with a significance level of 0.05. Anova was performed using Prism (GraphPad, Boston, USA).

## Results

### Patient Cohort

Twenty-five subjects met the inclusion criteria for this retrospective study. Demographic data of the patients are presented in Table 1. There was no major perioperative morbidity, and no postoperative mortality. The location of the distal landing zone was on Z4 for all patients. A debranching procedure was performed in 13 cases (52%), with 100% transpositions of the left subclavian artery, 46% debranching of the left carotid artery, and 62% transpositions of the brachiocephalic trunk.

**Table 1:** Clinical and procedure characteristics of the entire population (n =25).

| *Variable** | *Sample (N=25)* |
|---|---|
| ***Clinical Characteristics*** | |
| Male sex, n (%) | 20 (80%) |
| Age, median (range) | 72 (54 - 81) |
| BSA m² (range) | 2 (1.5-2.5) |
| Current smokers, n (%) | 16 (64%) |
| Former smokers, n (%) | 9 (36%) |
| Hypertension, n (%) | 24 (96%) |
| Diabetes, n (%) | 1 (4%) |
| Dyslipidemia, n (%) | 13 (52%) |
| CAOD | 10 (40%) |
| COPD | 10 (40%) |
| | |
| ***Procedure Characteristics*** | |
| *Aortic Zones* | |
| Z4 | 5(20%) |
| Z3 | 9(36%) |
| Z2 | 1(4%) |
| Z1 | 3(12%) |
| Z0 | 7 (28%) |
| *Procedure* | |
| TEVAR alone | 12(48%) |
| Debranching | 13 (52%) |
| *Number Devise* | 3.9 (range 1 to 4) |
| *Proximal Dialeter Device* | 39 mm (range 34 – 45) |
| *Distal Diameter Device* | 37 mm (range 32 – 45) |
| *Stent-graft diameter* | |
| <40 mm | 15 (60%) |
| >40 mm | 10 (40%) |
| *Length Aorte Covered* | 207.2 mm (range 127 - 389) |
| *TEVAR Oversizing* | 18 % (range 6.58% to 34. 39%) |
| <40 mm | 15 (60%) |
| >40 mm | 10 (40%) |

BSA = body surface area; CAOD = coronary artery occlusive disease; COPD = chronic occlusive pulmonary disease; TEVAR= thoracic endovascular aortic repair.

*Continuous data are described as medians (interquartile range [IQR]) and categoric data as numbers (%)

Seventeen patients were included in FAG. Eight patients required an aortic reintervention during follow-up due to endoleaks (Ia n=1; Ib n=2; Ia +Ib n=1; III n=2; Ib +III n=2) and were included in UBG. All surgical intervention were endovascular with the addition of at least one stent graft. The secondary procedures were performed for one patient after 12 months, for one patient after 24 months and for 6 patients after 36 months following elective TEVAR.

### Geometrical Parameters

All available CTA have been analysed and examples of centrelines evolution over time are provided in Figure 2. The mean time to obtained a manual segmentation of the aorta and to compute these informations for one patient over several time points were 8.3±2hours.

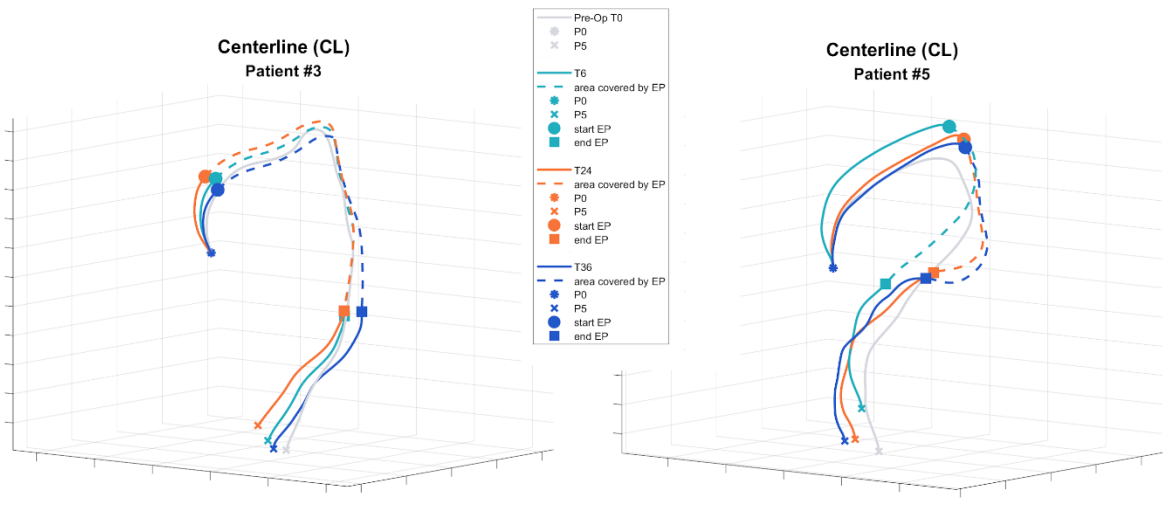


**Figure 2.** Example of centerline evolution on two different patients: one from the FAG (left graph) and one from the UBG (right graph).

### a. Geometrical Parameter at Each Time Points (Table 2)

L3_4 in UBG showed a higher value compared to FAG at 6 month (323.3±22.7 mm vs 296.7±11.9; $p<0.05$) as well as for later time points and was predictive of poor outcome, regardless of the post-operative time (OR=1.19, $CI_{95\%}$=[1.04;1.50]; 57.76 $CI_{95\%}$=[2.38;>1000]; 1.28 $CI_{95\%}$=[1.05;1.89], for T6, T24 and T36 respectively). Remarquably, L4 alone follow the same pattern and increasement of its value was predictive of poor outcome regardless of post-operative time. L3_4 and L4 showed the ability to predict unfavorable evolution earlier than Daneurysm. Daneurysm was significantly higher in UBG compared with FAG at T24 (69.2±11.0mm vs 59.3±9.6mm; $P<0.05$) and was linked to a risk of poor outcome at T24 (OR=1.14 ($CI_{95\%}$=[1.01;1.30]) and T36 (OR=1.15, $CI_{95\%}$=[1.03;1.33]). L_Atot was predictive of poor outcome since T24 (OR=1.05 $CI_{95\%}$=[1.01;1.10]) and at T36 (OR=1.03 ($CI_{95\%}$=[1.00;1.07]). $adnadn$ was higher in UBG and predictive of poor outcome at T24 and T36. The vast majority of the other parameter did not showed and significance or significance at only one time point which is difficult to interpret and probably need more data.

**Table 2:** Assessment of risk of a patient switching to unfavorable group at T0 and at each post-operative follow-up.

| | T0 | | | T6 | | | T24 | | | T36 | | |
|---|---|---|---|---|---|---|---|---|---|---|---|---|
| **Parameters** | **OR** | **95% Confidence Interval (CI)** | | **OR** | **95% Confidence Interval (CI)** | | **OR** | **95% Confidence Interval (CI)** | | **OR** | **95% Confidence Interval (CI)** | |
| | | **CI -** | **CI +** | | **CI -** | **CI +** | | **CI -** | **CI +** | | **CI -** | **CI +** |
| **Angles αi - °** | | | | | | | | | | | | |
| αpn | 1,00 | 0,91 | 1,08 | 1,00 | 0,95 | 1,05 | 0,93 | 0,85 | 1,00 | 0,96 | 0,88 | 1,02 |
| αdn | 1,00 | 0,92 | 1,09 | 1,04 | 0,99 | 1,11 | **1,07** | **1,00** | **1,15** | **1,12** | **1,02** | **1,27** |
| α_EP | 1,01 | 0,99 | 1,04 | 1,00 | 0,97 | 1,03 | 1,01 | 0,98 | 1,05 | 1,01 | 0,98 | 1,05 |
| α_ATot | 1,00 | 0,96 | 1,04 | 0,98 | 0,93 | 1,03 | 1,02 | 0,97 | 1,07 | 1,00 | 0,95 | 1,04 |
| α0 | 1,02 | 0,98 | 1,08 | **1,11** | **1,01** | **1,24** | **1,12** | **1,01** | **1,28** | 0,99 | 0,93 | 1,05 |
| α0+α1+α2 | 0,98 | 0,92 | 1,04 | 1,15 | 0,96 | 1,53 | 1,09 | 0,96 | 1,32 | 0,94 | 0,82 | 1,06 |
| α1 | 1,09 | 0,93 | 1,31 | 1,00 | 0,80 | 1,24 | **2,07** | **1,17** | **5,86** | 1,34 | 0,96 | 2,06 |
| α1+α2 | 1,01 | 0,93 | 1,10 | 0,95 | 0,81 | 1,07 | 0,92 | 0,73 | 1,08 | 1,02 | 0,87 | 1,22 |
| α2 | 1,03 | 0,95 | 1,11 | 0,94 | 0,80 | 1,06 | 0,92 | 0,75 | 1,06 | 0,93 | 0,76 | 1,07 |
| α3 | 1,01 | 0,97 | 1,06 | **1,08** | **1,00** | **1,22** | 1,01 | 0,96 | 1,08 | 1,02 | 0,97 | 1,09 |
| α3+α4 | 0,98 | 0,93 | 1,03 | 1,00 | 0,94 | 1,06 | 0,97 | 0,88 | 1,03 | 1,01 | 0,95 | 1,06 |
| α4 | 0,97 | 0,90 | 1,03 | 0,97 | 0,92 | 1,02 | 0,97 | 0,91 | 1,02 | 0,99 | 0,93 | 1,05 |
| **Length (Li) - mm** | | | | | | | | | | | | |
| Lpn | 0,80 | 0,80 | 1,13 | **1,23** | **1,03** | **1,59** | 1,03 | 0,89 | 1,19 | 0,93 | 0,79 | 1,06 |
| Ldn | 1,07 | 0,93 | 1,24 | 1,10 | 0,99 | 1,25 | 1,17 | 0,97 | 1,49 | 0,90 | 0,76 | 1,03 |
| L_EP | 0,99 | 0,96 | 1,01 | 1,00 | 0,99 | 1,02 | 1,00 | 0,98 | 1,02 | 1,01 | 0,99 | 1,02 |
| L_ATot | 1,00 | 0,97 | 1,03 | 1,03 | 0,99 | 1,08 | **1,05** | **1,01** | **1,10** | **1,03** | **1,00** | **1,07** |
| L0 | 1,03 | 0,94 | 1,15 | 1,02 | 0,97 | 1,08 | 1,03 | 0,96 | 1,11 | 0,98 | 0,90 | 1,06 |
| L0+L1+L2 | 1,03 | 0,96 | 1,11 | 1,00 | 0,91 | 1,11 | 0,95 | 0,82 | 1,05 | **0,82** | **0,64** | **0,99** |
| L1 | 1,00 | 0,85 | 1,19 | 0,95 | 0,78 | 1,15 | 1,00 | 0,74 | 1,39 | 1,03 | 0,84 | 1,28 |
| L1+L2 | 1,03 | 0,94 | 1,15 | 0,96 | 0,80 | 1,15 | 0,95 | 0,72 | 1,23 | 1,13 | 0,88 | 1,54 |
| L2 | 1,03 | 0,93 | 1,13 | 0,91 | 0,68 | 1,16 | 0,66 | 0,26 | 1,14 | **0,33** | **0,06** | **0,89** |
| L3 | 0,94 | 0,86 | 1,01 | 1,05 | 0,95 | 1,18 | 1,02 | 0,88 | 1,21 | 1,02 | 0,93 | 1,14 |
| L3+L4 | 1,00 | 0,96 | 1,04 | **1,19** | **1,04** | **1,50** | **57,76** | **2,38** | **>1000** | **1,28** | **1,05** | **1,89** |
| L4 | 1,02 | 0,98 | 1,07 | **1,06** | **1,00** | **1,14** | **1,11** | **1,03** | **1,24** | **1,05** | **1,00** | **1,11** |
| **Tortuosity index (TI)** | | | | | | | | | | | | |
| TI_EP | 16,07 | 0,03 | >1000 | 0,62 | 0,00 | >100 | 12,53 | 0,15 | 2297,32 | 7,23 | 0,08 | >1000 |
| TI_ATot | **0,04** | **0,00** | **0,77** | 0,39 | 0,02 | 6,47 | 0,31 | 0,02 | 2,76 | 0,71 | 0,08 | 4,94 |
| TI0+TI1+TI2 | 4,55 | 0,00 | >1000 | >1000 | 0,00 | >1000 | >1000 | 0,00 | >1000 | 0,05 | 0,00 | >1000 |
| TI3+TI4 | 0,00 | 0,00 | 3,54 | 98,03 | 0,00 | >1000 | 90,28 | 0,01 | >1000 | >100 | 0,01 | >1000 |
| **Diameter (D) - mm** | | | | | | | | | | | | |
| Daneurysm | 1,01 | 0,92 | 1,11 | 1,05 | 0,95 | 1,15 | **1,14** | **1,01** | **1,30** | **1,15** | **1,03** | **1,33** |
| Dpn | 1,12 | 0,87 | 1,47 | **1,20** | **1,01** | **1,51** | 1,18 | 0,96 | 1,51 | 1,20 | 0,99 | 1,55 |
| Ddn | 0,95 | 0,68 | 1,28 | 1,08 | 0,88 | 1,36 | 1,06 | 0,82 | 1,36 | 1,00 | 0,80 | 1,25 |
| D0 | 0,94 | 0,70 | 1,19 | 1,05 | 0,87 | 1,27 | 1,01 | 0,82 | 1,26 | 0,97 | 0,77 | 1,22 |
| D1 | 1,01 | 0,77 | 1,33 | 1,03 | 0,78 | 1,37 | 1,05 | 0,76 | 1,46 | 1,09 | 0,76 | 1,62 |
| D2 | 1,05 | 0,99 | 1,12 | 0,86 | 0,54 | 1,16 | 0,90 | 0,65 | 1,21 | 0,80 | 0,46 | 1,14 |
| D3 | 0,97 | 0,87 | 1,07 | 1,03 | 0,96 | 1,10 | 1,07 | 1,00 | 1,18 | **1,07** | **1,00** | **1,16** |
| D4 | 1,15 | 0,95 | 1,44 | 1,08 | 0,92 | 1,28 | 1,22 | 0,99 | 1,65 | 1,05 | 0,91 | 1,23 |

### a. Temporal evolution of geometrical parameters

Angle α3_4 increases by a mean value of 23° and length L3_4 increases by a mean value of 22mm in UBG, whereas in FAG, the evolution is negligible (-1° and 0.01mm respectively). This analysis showed that the temporal evolution of several parameters were able to predict unfavourable evolution earlier that diameters and consistently over follow-up. The decrease of α2 over time and on the opposite side the increase of α3_4 are predictive of bad evolution and showed that the unfavorable aortic remodelling is highly dependent of the anatomy of the thoracic aorta. Interestingly evolution of the aorta length over time showed consistent result with a decrease of L2 and the increase of L3_L4 were predictive of poor outcome. The tortuosity of the distal part of the aorta showed as well interesting and early information to predict unfavourable evolution. (Table 3 and Figure 3).

| | Δ T0 vs T6 | | | ΔT0 vs T24 | | | Δ T0 vs T36 | | |
|---|---|---|---|---|---|---|---|---|---|
| **Parameters** | **β1** | **95% Confidence Interval (CI)** | | **β1** | **95% Confidence Interval (CI)** | | **β1** | **95% Confidence Interval (CI)** | |
| | | **CI -** | **CI +** | | **CI -** | **CI +** | | **CI -** | **CI +** |
| **Angles αi - °** | | | | | | | | | |
| αpn | 3,3 | -18,3 | 25,1 | -14,4 | -33,2 | 4,5 | 0,6 | -16,9 | 18,2 |
| αdn | -0,6 | -20,6 | 19,7 | 6,9 | -14,6 | 28,7 | **20,2** | **6,7** | **33,8** |
| α_EP | -11,1 | -37,5 | 15,6 | 5,5 | -29,6 | 41,0 | **-30,7** | **-53,4** | **-7,9** |
| α_ATot | 11,7 | -9,3 | 32,9 | 19,1 | -8,5 | 46,9 | 15,1 | -6,2 | 36,5 |
| α0 | -3,4 | -21,9 | 15,3 | -3,1 | -25,1 | 19,1 | -18,6 | -42,4 | 5,6 |
| α0+α1+α2 | -1,6 | -14,8 | 11,8 | -2,4 | -14,4 | 9,6 | -12,9 | -26,5 | 0,9 |
| α1 | 1,8 | -0,4 | 4,0 | **2,4** | **0,3** | **4,5** | **3,3** | **0,3** | **6,5** |
| α1+α2 | **-11,1** | **-17,7** | **-4,4** | **-8,8** | **-12,5** | **-5,1** | -3,8 | -8,1 | 0,5 |
| α2 | **-9,4** | **-16,3** | **-2,4** | **-9,8** | **-13,9** | **-5,6** | **-7,9** | **-12,8** | **-3,0** |
| α3 | **21,1** | **13,9** | **28,5** | 8,9 | -7,3 | 25,3 | 7,5 | -9,6 | 24,7 |
| α3+α4 | **24,0** | **9,8** | **38,3** | **13,4** | **5,0** | **21,8** | **25,5** | **11,4** | **39,6** |
| α4 | 0,6 | -11,5 | 12,8 | -1,6 | -17,8 | 14,7 | 5,1 | -6,2 | 16,5 |
| **Length (Li) - mm** | | | | | | | | | |
| Lpn | 4,9 | -3,7 | 13,5 | -0,9 | -8,2 | 6,6 | -0,7 | -6,8 | 5,5 |
| Ldn | -1,8 | -12,1 | 8,7 | -0,5 | -7,9 | 6,9 | -8,0 | -16,4 | 0,5 |
| L_EP | -15,7 | -45,1 | 14,1 | -9,3 | -41,0 | 22,7 | -15,7 | -46,7 | 15,6 |
| L_Atot | **16,8** | **1,8** | **32,0** | **31,9** | **10,3** | **53,7** | **38,3** | **15,2** | **61,7** |
| L0 | 1,1 | -10,2 | 12,6 | 0,6 | -10,4 | 11,6 | -2,7 | -14,6 | 9,4 |
| L0+L1+L2 | -8,5 | -20,3 | 3,4 | **-12,9** | **-24,1** | **-1,7** | **-19,5** | **-28,1** | **-10,8** |
| L1 | 1,2 | -0,4 | 2,8 | **3,8** | **1,2** | **6,6** | **6,8** | **2,6** | **11,1** |
| L1+L2 | **-7,2** | **-11,1** | **-3,2** | -3,2 | -6,3 | 0,0 | 0,2 | -4,9 | 5,4 |
| L2 | **-8,0** | **-12,3** | **-3,6** | **-8,2** | **-12,1** | **-4,2** | **-9,2** | **-12,0** | **-6,3** |
| L3 | **33,0** | **22,3** | **43,8** | **22,5** | **14,9** | **30,2** | **23,0** | **8,9** | **37,3** |
| L3+L4 | **22,0** | **15,2** | **28,9** | **48,4** | **32,2** | **64,8** | **58,9** | **38,6** | **79,3** |
| L4 | 5,7 | -9,1 | 20,7 | **19,1** | **4,4** | **34,0** | **24,8** | **5,2** | **44,6** |
| **Tortuosity index (TI)** | | | | | | | | | |
| TI_EP | 0,0 | -0,2 | 0,1 | 0,1 | -0,1 | 0,3 | 0,0 | -0,2 | 0,1 |
| TI_ATot | 0,1 | -0,2 | 0,4 | 0,1 | -0,2 | 0,4 | 0,2 | 0,0 | 0,5 |
| TI0 TI1+TI2 | 0,0 | -0,1 | 0,0 | 0,0 | -0,1 | 0,0 | -0,1 | -0,1 | 0,0 |
| TI3+TI4 | **0,1** | **0,1** | **0,2** | **0,2** | **0,1** | **0,3** | **0,2** | **0,1** | **0,3** |
| **Diameter (D) - mm** | | | | | | | | | |
| Daneurysm | -2,2 | -6,3 | 1,9 | **11,0** | **3,0** | **19,0** | **13,2** | **2,0** | **24,5** |
| Dpn | 0,7 | -8,5 | 9,9 | **5,8** | **2,0** | **9,5** | **3,9** | **0,5** | **7,4** |
| Ddn | 4,6 | -0,2 | 9,5 | **7,6** | **1,5** | **13,7** | **6,8** | **4,1** | **9,6** |
| D0 | -1,5 | -4,0 | 1,1 | -0,8 | -2,8 | 1,3 | -0,3 | -2,9 | 2,3 |
| D1 | 0,3 | -1,6 | 2,2 | 0,2 | -1,2 | 1,6 | 1,7 | -0,1 | 3,6 |
| D2 | -1,3 | -4,3 | 1,7 | -0,3 | -2,9 | 2,3 | -1,4 | -3,4 | 0,5 |
| D3 | 0,3 | -8,2 | 8,8 | -0,8 | -5,2 | 3,7 | 5,9 | -3,2 | 15,2 |
| D4 | -2,0 | -4,4 | 0,3 | -1,5 | -4,3 | 1,3 | 0,0 | -3,8 | 3,8 |

**Table 3:** Temporal evolution of parameters between T0 and each post-operative follow-up and statistical analysis.

Finally, evolution of Daneurysm over time is predictive of bad outcomes since T24 wile several other parameter explained above showed earlier significance.

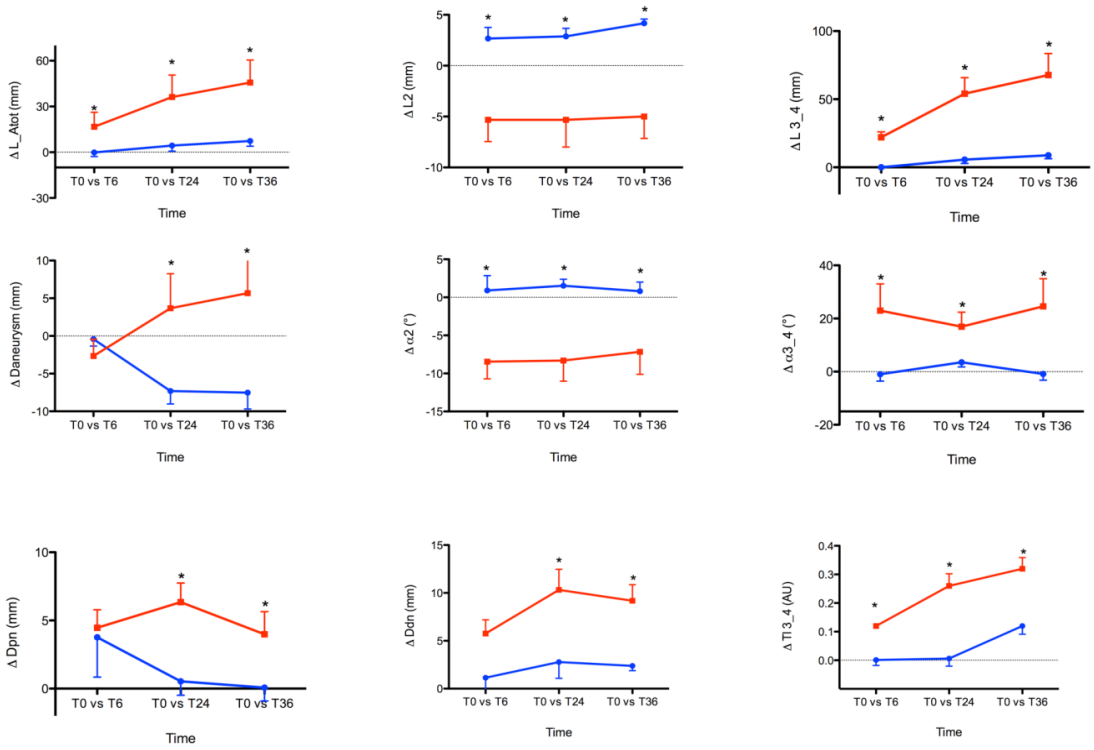


**Figure 3.** Graphs plotting the difference between T0 and successive time points, for the 9 morphological parameters of interest. Blue lines are FAG evolution, red lines are UBG evolution.

**Discussion**

The main findings of the present study are:

**1)** The described method to assess geometrical parameter is feasible but time consuming.

**2)** Several geometrical parameters showed the ability to discriminate 6 months after TEVAR patients that will show bad aortic outcomes.

Most clinical studies consider a few parameters at one fixed point in the post-operative follow-up [12,13]; a short postoperative period and/or patients suffering from a variety of pathologies [14-16]. Temporal evolution of aortic length differs significantly between the two groups once a comparative analysis between T0 and T6 is performed. These results are consistent with those of Spinella et al. [17] who showed that the aortic length along the centerline between the aortic root and celiac artery increased when 1-month and 1-year follow-up CTs were compared. A recent study performed by Chen et al. [18] on the lengthening of the thoracic aorta in heterogeneous pathologies showed a progressive increase after TEVAR, with lengthening from the innominate artery to the celiac artery at a mean rate of 1.7mm per year. L_Atot also shows a significantly different temporal evolution in the two groups between T0 and T24 and between T0 and T36. Aortic elongation in aneurysmal patients has already been noted in previous studies [12,16]. The present study, based on long-term regular yearly follow-up, found an increase in centerline length from the subclavian artery to the coeliac trunk, particularly in UBG evolution. This could be due to progressive and continuous elongation, even in patients who will not develop endoleak. We believe that the interaction of the endoprosthesis with the aortic wall, together with wall aging, modifies the structure of the media, leading to slow and progressive elongation.

The present study showed that the tortuosity of the descending aorta was associated with poor outcome. This result was in line with previous study. Chen et al. [19] demonstrated that high tortuosity of the thoracic aorta is associated with higher rates of endoleaks and stroke, and lower survival in patients undergoing TEVAR for atherosclerotic aneurysm, through a follow-up lasting 29±26 months. Higher tortuosity of the aorta is likely to lead to a higher rate of endoleaks because a tortuous aorta provides a poor fit for stent grafts, leaving a space between the endoprosthesis and the aortic wall. Aneurysm diameter is predictive of poor outcome at T24 and T36 but not at T6. On the contrary, the lengths and angles of the aortic arch (Z2) and of the descending aorta (Z3_Z4) are found to change significantly in both groups between T0 and T6. This tends to show that the diameter seems to be the latest parameter to be impacted by post TEVAR remodeling. Moreover, concerning the lengths and angles of the aortic arch (Z2) and of the descending aorta (Z3_Z4), most of the significant differences in evolution found between T0 and T6 remain valid when analyzing evolution between T0 and T24 or between T0 and T36. This shows that evolution of these key parameters over time follows a consistent pattern.

Adaptation and interaction of the vessel with the endoprosthesis in the first months should be closely monitored. Regardless of the native morphology of the aorta, choosing a device whose design accommodates a complex geometry might be of prime importance. The main limitation of the study regards the use of the semimanual methods to identify the external wall of the aneurysm which could be affected by inter-operator errors. Furthermore, the presented method is time consuming. Although the number of enrolled patients is small for that purpose bayesian statistical studies have been used. Finally, there is an inhomogeneity of the proximal landing zone in our study that might have introduce heterogeneity in data analysis.

## Conclusion

The present study suggests that the increase in tortuosity (TI3_4), increased angulation (α3_4) and increase in length (L3_4) of the descending thoracic aorta discriminates between the favorable and the unfavorable group earlier that maximal diameter and maximal diameter evolution. Artificial intelligence technique might be an opportunity to bring such measured in the clinical arena to be able to assess these parameters in larger population.

## Supplementary Materials:

Supplemental Appendix 1. CTA protocol Non-ionic iodinated contrast medium (between 120 and 150 ml) was injected through an antecubital vein at a rate of 4-6 mL/s, tailored to the body weight of the patient. Three acquisitions were carried out for each patient: an acquisition without injection of contrast medium, then one with injection of contrast medium at the arterial phase using automated bolus triggering, and a delayed acquisition (90 seconds later) for assessment of endoleaks. Slice thickness varied between 0.6mm for the arterial phase and late phase acquisitions and 3mm for the non-enhanced acquisition.

Supplemental Appendix 2. Bayesian Methods: Bayesian and frequentist approaches are still subject of debate in statistics. However, Bayesian methods are notably an attractive alternative for better trials with cohort of small sample size [20-22].The two models, in which a response variable $Y_i$ is related to one or more explanatory variables $Xi_1,\ldots Xi_q$ for a random sample of n individuals, are:

Linear regression: $Y_i = \beta_0 + \beta_1 X_{i1} + \beta_2 X_{i2} + \cdots + \beta_q X_{iq} + \varepsilon_i$ (Equation 1)

Logistic regression $P(Y_i = 1) = \frac{e^{\beta_0+\beta_1 X_{i1}+\beta_2 X_{i2}+\cdots+\beta_q X_{iq}+\varepsilon_i}}{1+e^{\beta_0+\beta_1 X_{i1}+\beta_2 X_{i2}+\cdots+\beta_q X_{iq}+\varepsilon_i}}$ (Equation 2)

where i is the number of observations (i ϵ [1,n]), q the number of explanatory variables and $\varepsilon_i$ an error term representing random sampling noise. Typically, $\varepsilon_i$ is assumed to be normally distributed with mean 0 and variance $\sigma^2\sigma^2$, i.e $\varepsilon_i \sim N(0,\sigma^2)$, and $\varepsilon_i$ and $\varepsilon_j$ are independent for $i \neq j$. In the Bayesian approach, probability distributions are used to quantify uncertainty. Thus, in contrast to the frequentist approach, a joint probability model for response and parameters is specified conditional on the parameters $(\beta_j, X_{ij})$. Writing $X_i = (X_{i1}, X_{i2}, \ldots, X_{iq})$ and $\beta = (\beta_1, \beta_2, \ldots, \beta_q)$, after observing the sample data and for each response variable $Y_i$, the prior distribution ($P(\beta|X_i)$) is updated by the empirical data applying the Bayes theorem

$P(\beta|Y_i, X_i) = \frac{P(Y_i|\beta, X_i) \times P(\beta|X_i)}{P(Y_i|X_i)}$ (Equation 3)

which yields the so-called posterior distribution of the parameters $(\beta, X_i)$, with ($P(Y_i|\beta, X_i)$) the likelihood of the data. Due to the absence of any prior knowledge in this study, vague priors are used. For regression coefficients, the prior distribution is a very broad normal distribution, with a mean of zero and a large enough standard deviation ($10^6$).

The Markov Chain Monte Carlo (MCMC) sampling method was used to approximate the posterior distribution. The end result of Bayesian Linear Modeling is not a single estimate for the model parameters, but a distribution that can be used to make inferences about new observations [23].

The Bayesian logistic regression defined by equation 2 is performed to evaluate the associations between unfavorable

outcomes and geometrical explanatory variables at preoperative (T0) and postoperative stages (T6, T24, and T36).

**Temporal evolution.** The evolution of each morphological and geometrical parameter (outcome) was compared between favorable (FAG) and unfavorable (UBG) groups (explanatory variable). Evolution was determined by computing the differences between the postoperative stages (T6, T24, and T36) and the preoperative stage (T0).

For subject i our model is determined using equation 1 as follows:

$$Y_{iTj} = \Delta_{iTj} = V_{Tj} - V_{T0} = \beta_0 + \beta_1 \times \text{Group} \quad \text{(Equation 4)}$$

where $V_{Tj}$ is the morphological or geometrical parameter at postoperative stage Tj (j=6, 24, or 36) ; Group is set at 1 for the UBG and 0 otherwise.

If $\beta_1$ is significantly positive, the evolutionary parameter increases more in UBG than in FAG. Conversely, if $\beta_1$ is significantly negative, the evolutionary parameter decreases more in UBG than in FAG. The 95% confidence interval (CI) is calculated for the $\beta_1$ coefficient of group variable. If the confidence interval does not include the null value, we conclude that there is a statistically significant difference in evolution between the groups. To verify the goodness of fit of our model, Geweke's convergence diagnostic was conducted [24] for the β coefficients by calculating Z-scores and the corresponding p-values. The p-values were all higher than 0.35, indicating adequate mixing and convergence.

**Funding:** This research received no external funding.

**Institutional Review Board Statement:** The retrospective study was conducted according to the guidelines of the Declaration of Helsinki, and approved by the Local Ethics Committee of AP-HM in Marseille

**Informed Consent Statement:** The ethics committee waived the need for individual written informed consent.

**Data Availability Statement:** The data underlying this article will be shared upon reasonable request to the corresponding author.

**Conflicts of Interest:** The authors declare no conflict of interest.

## References

1. Geisbüsch P, Kotelis D, Hyhlik-Dürr A, Hakimi M, Attigah N, et al. (2010) Endografting in the Aortic Arch-Does the Proximal Landing Zone Influence Outcome? Eur J Vasc Endovasc Surg 39: 693-699.
2. Mokashi SA, Svensson LG (2019) Guidelines for the Management of Thoracic Aortic Disease in 2017. Gen Thorac Cardiovasc Surg 67: 59-65.
3. Virmani R, Avolio AP, Mergner WJ, Robinowitz M, Herderick EE, et al. (1991) Effect of Aging on Aortic Morphology in Populations with High and Low Prevalence of Hypertension and Atherosclerosis. Comparison between Occidental and Chinese Communities. Am J Pathol 139: 1119-1129.
4. O'Rourke MF, Hashimoto J (2007) Mechanical Factors in Arterial Aging: A Clinical Perspective. J. Am. Coll. Cardiol 50: 1-13.
5. Weisbecker H, Pierce DM, Regitnig P, Holzapfel GA (2012) Layer-Specific Damage Experiments and Modeling of Human Thoracic and Abdominal Aortas with Non-Atherosclerotic Intimal Thickening. J Mech Behav Biomed Mater 12: 93-106.
6. Criado FJ (2010) Mapping the Aorta: A New Look at Vascular Anatomy in the Era of Endograft Repair. J Endovasc Ther 17: 68-72.
7. Ishimaru S (2004) Endografting of the Aortic Arch. J Endovasc Ther 11: II62- II71.
8. Langs G, Paragios N, Desgranges P, Rahmouni A, Kobeiter H (2011) Learning Deformation and Structure Simultaneously: In Situ Endograft Deformation Analysis. Medical Image Analysis 15: 12-21.
9. Domanin M, Bissacco D, Romarowsky RM, Conti M, Auricchio F, et al. (2021) Drag Forces after Thoracic Endovascular Aortic Repair. General Review of the Literature. Annals of Vascular Surgery 75: 479-488.
10. Ranney DN, Cox ML, Yerokun BA, Benrashid E, McCann RL, et al. (2018) Long-Term Results of Endovascular Repair for Descending Thoracic Aortic Aneurysms. J Vasc Surg 67: 363-368.
11. Ammar CP, Larion S, Ahanchi SS, Lavingia KS, Dexter DJ, et al. (2016) Anatomic Severity Grading Score for Primary Descending Thoracic Aneurysms Predicts Procedural Difficulty and Aortic-Related Reinterventions after Thoracic Endovascular Aortic Repair. J Vasc Surg 64: 912-920.e1.
12. Naguib NNN, Zima B, Nour-Eldin NEA, Gruber-Rouh T, Fischer S, et al. (2016) Long-Term Changes in Aortic Length after Thoracic Endovascular Aortic Repair. Journal of Vascular and Interventional Radiology 27: 181-187.
13. Mestres G, Garcia ME, Yugueros X, Urrea R, Tripodi P, et al. (2017) Aortic Arch and Thoracic Aorta Curvature Remodeling after Thoracic Endovascular Aortic Repair. Ann Vasc Surg 38: 233-241.
14. Midulla M, Moreno R, Negre-Salvayre A, Nicoud F, Pruvo JP, et al. (2014) Impact of Endografting on the Thoracic Aortic Anatomy: Comparative Analysis of the Aortic Geometry before and after the Endograft Implantation. Cardiovasc Intervent Radiol 37: 69-76.
15. Qing K, Yiu W, Cheng SWK (2012) A Morphologic Study of Chronic Type B Aortic Dissections and Aneurysms after Thoracic Endovascular Stent Grafting. J Vasc Surg 55: 1268-1275.
16. Alberta HB, Takayama T, Panthofer A, Cambria RP, Farber MA, et al. (2018) Thoracic Endovascular Aortic Repair Migration and Aortic Elongation Differentiated Using Dual Reference Point Analysis. Journal of Vascular Surgery 67: 382-388.
17. Spinella G, Finotello A, Conti M, Faggiano E, Gazzola V, et al. (2019) Assessment of Geometrical Remodelling of the Aortic Arch after Hybrid Treatment. European Journal of Cardio-Thoracic Surgery 55: 1045-1053.
18. Chen CK, Chou HP, Chang YY, Shih CC (2020) Elongation of the Aorta after Thoracic Endovascular Aortic Repair: A Longitudinal Study. IJERPH 17: 1205.

**19.** Chen CK, Liang IP, Chang HT, Chen WY, Chen IM, et al. (2014) Impact on Outcomes by Measuring Tortuosity with Reporting Standards for Thoracic Endovascular Aortic Repair. J Vasc Surg 60: 937-944.

**20.** Henderson NC, Louis TA, Wang C, Varadhan R (2016) Bayesian Analysis of Heterogeneous Treatment Effects for Patient-Centered Outcomes Research. Health Serv Outcomes Res Method 16: 213-233.

**21.** Jack-Lee J, Chu CT (2012) Bayesian Clinical Trials in Action. Statist Med 31: 2955-2972.

**22.** Vande-Schoot R, Broere JJ, Perryck KH, Zondervan-Zwijnenburg M, vanLoey NE (2015) Analyzing Small Data Sets Using Bayesian Estimation: The Case of Posttraumatic Stress Symptoms Following Mechanical Ventilation in Burn Survivors. European Journal of Psychotraumatology 6: 25216.

**23.** Gelman A, Rubin DB (1992) Inference from Iterative Simulation Using Multiple Sequences. Statist Sci 7: 451-511.

**24.** Geweke J (1992) Evaluating the Accuracy of Sampling-Based Ap-Proaches to the Calculation of Posterior Moments. In: Bayesian Statistics. In Bayesian Statistics; Oxford: Oxford University Press 4: 169-193.